Harmonic Compensation Using On-Line Bacterial Foraging Optimization Based Three-Phase Active Power Filter

G. El-Saady
Elect. Eng. Depart.
Assiut University
Faculty of Eng., Assiut
Egypt
gaber_1@yahoo

Abou-Hashima El-Sayed
Elect. Eng. Depart.
Minia University
Faculty of Eng., Minia
Egypt
dr_mostafa555@yahoo

E. A. Ebrahim
Power Elect. Depart.
Elect. Research Institute
Dokki., Cairo
Egypt
essamudin@yahoo

H. I. Abdul-Ghaffar
PHD graduate student
Minia University
Faculty of Eng., Minia
Egypt
abdelghafar_ibrahim@yahoo

***Abstract*:-** The active power filter has gained much more attention because of its effective performance to mitigate the harmonics. This paper presents shunt active power filter (SAPF) controlled by PI controller to compensate the harmonics. Also, it introduces a new artificial intelligent technique called Bacterial Foraging Optimization to optimize the parameters of the PI-controller through on-line self-adaptive self-tuning algorithm. This robust control scheme of the system makes improvement in the behavior of the active filter to eliminate the harmonic currents which occurred by the nonlinear loads in the electric grid. The hysteresis non-linear current control method is used to generate the pulse gate required to drive PWM current-controlled voltage-source inverter of SAPF. Matlab/Simulink software package is used as a simulation to test and simulate the proposed system. Through the simulation results, it is observed that the response of the PI controller based on-line bacteria foraging optimization is quite satisfactory.

Key words:- Active Power Filter, PI controller, Bacterial Foraging Optimization, Hysteresis Current Control.

1 Introduction

Nowadays, using of nonlinear industry loads based on power electronic elements increases such as: industrial equipments (welding machines, arc furnaces, rectifiers and motors), offices equipments (computers and photocopiers), domestic devices (TVs, micro-wave furnaces and lighting) and power inverters. This leads to high current harmonics and low power factor which lead to power quality problems. The harmonic currents spread into electric grid and interact adversely with a wide range of power system equipments, control systems, protection circuits, and other harmonic sensitive loads which leads to negative effect on them.

In order to face the harmonic problems, passive filters were used to eliminate the harmonics and improve the power factor of the supply. These passive filters have disadvantages such as: resonance, the large size, insufficient fitness for large bands of harmonic frequencies which imply using of many filters, fixed compensation (very low flexibility for load variations that lead to new filter design for each load variation) [1]. During the last three decades, the concept of active power filter (APF) has been introduced and many publications have represented in this subject [2-5]. To reduce the size of SAPF, several approaches such as, multistep inverters and hybrid filters are reported [6]. Also, Many control techniques such as instantaneous power theory [7], flux based controllers [8], and notch filters [9] have been introduced. Most of these control schemes are difficult to implement and require various transformations.

This research presents a new algorithm based on the foraging behavior of *E-coli* bacteria in the humane intestine, to optimize the coefficients of the PI controller which lead to generate effective filter currents that eliminate harmonics. The BFO scheme has been proposed by Passino [10], it incorporated by Mishra and used for many publications for optimization [11–24]. The PI controller based bacterial foraging technique converges faster than the classical PI controller to reach the global minimum optimal solution. The hysteresis current control method is used to generate the gate pulses required for the SAPF by comparing between the actual currents and the reference currents.

The proposed system is tested with non-linear load fed from the source through uncontrolled three phase bridge rectifier.

The proposed system is known as PI-BFO controlled SAPF.

This paper will be organized as follows: The system model is presented in section 2. In section 3, the control scheme is introduced while objective function is given in section 4. Simulation results and discussions are obtained in section 5. Some concluding remarks are highlighted in section 6. About twenty five research publications are reviewed, discussed, classified, and appended for a quick reference.

2 System Model

The system under study comprises of three-phase source voltages, non-linear load and active power filter as shown in Figure 1. The components of the system are analyzed separately and integrated to develop the complete model for simulation.

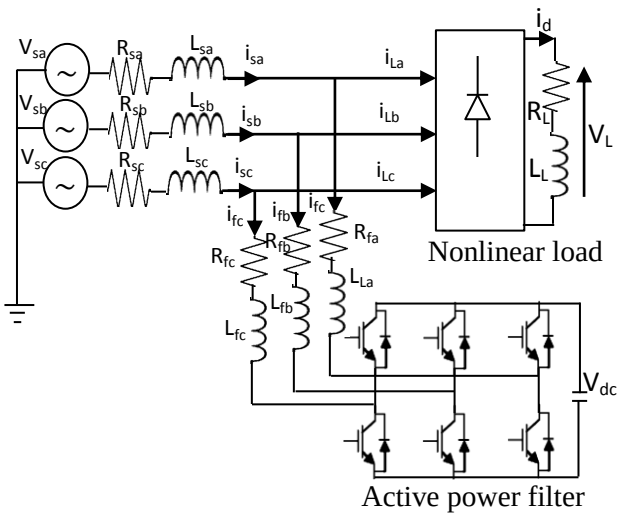

Fig. 1 Block diagram of the system with SAPF

2.1 Three-Phase Source Voltages

The three-phase source voltages under ideal conditions can be expressed as

$$\left.\begin{aligned} V_{sa} &= V_m \sin(\omega t) \\ V_{sb} &= V_m \sin(\omega t - 120) \\ V_{sc} &= V_m \sin(\omega t + 120) \end{aligned}\right\} \quad (1)$$

Where, V_m is the peak value of the source voltage and ω is the frequency of the AC source in rad/sec. The three-phase source currents are given by:

$$\left.\begin{aligned} i_{sa} &= i_{fa} + i_{La} \\ i_{sb} &= i_{fb} + i_{Lb} \\ i_{sc} &= i_{fc} + i_{Lc} \end{aligned}\right\} \quad (2)$$

Where (i_{sa}, i_{sb} and i_{sc}) are the three-phase source currents, (i_{fa}, i_{fb} and i_{fc}) are the three phase APF currents and (i_{La}, i_{Lb} and i_{Lc}) are the three phase load currents.

2.2 Nonlinear Load

The nonlinear load consists of three-phase uncontrolled diode bridge rectifier with inductive – resistive load. When the diodes are conducting , the AC source is connected to the load and the basic equation is:

$$2R_S\, i_d + 2L_S\, pi_d + V_L = V_S \quad (3)$$

Where, R_S and L_S are the resistance and the inductance of the AC source. V_L is the instantaneous voltage across the dc side and V_S is the source line voltage. 'p' is the differential operator (d/dt) and i_d is the current flowing from the AC source through the diodes.

$$\text{So, } pi_d = \frac{V_s - V_L - 2R_s i_d}{2L_s} \quad (4)$$

The three-phase load currents (i_{La}, i_{Lb} and i_{Lc}) are obtained using the magnitude of i_d and the sign according to the conducting diodes. When the diodes are not conducting the current i_d and its derivative will be zero.

2.3 Shunt Active Power Filter (SAPF)

The SAPF is composed of a standard three-phase voltage source inverter bridge with a DC bus capacitor to provide an effective current control. the controlled currents of the SAPF is given by differential equations as follow:

$$pi_{fa} = -\frac{R_f}{L_f} i_{fa} + \frac{V_{sa} - V_{fa}}{L_f} \quad (5)$$

$$pi_{fb} = -\frac{R_f}{L_f} i_{fb} + \frac{V_{sb} - V_{fb}}{L_f} \quad (6)$$

$$pi_{fc} = -\frac{R_f}{L_f} i_{fc} + \frac{V_{sc} - V_{fc}}{L_f} \quad (7)$$

Where, R_c and L_c are the resistance and the inductance of the SAPF. V_{sa}, V_{sb} and V_{sc} are the three-phase source voltages and i_{fa}, i_{fb} and i_{fc} are the three-phase SAPF currents. V_{fa}, V_{fb} and V_{fc} are three-phase SAPF voltages.

The DC capacitor current can be obtained in terms of phase currents (i_{fa}, i_{fb} and i_{fc}) and the pattern of switching devices (S_a, S_b and S_c).

$$i_{dc} = i_{fa} S_a + i_{fb} S_b + i_{fc} S_c \quad (8)$$

The DC side capacitor voltage can be given by

$$pV_{dc} = \frac{i_{fa}S_a + i_{fb}S_b + i_{fc}S_c}{C_{dc}} \quad (9)$$

The three-phase SAPF voltages can be given by:

$$\left.\begin{aligned} V_{fa} &= \frac{V_{dc}}{3}\,(2S_a - S_b - S_c) \\ V_{fb} &= \frac{V_{dc}}{3}\,(-S_a + 2S_b - S_c) \\ V_{fc} &= \frac{V_{dc}}{3}\,(-S_a - S_b + 2S_c) \end{aligned}\right\} \quad (10)$$

The main function of the proposed SAPF is eliminating harmonics occurring in power grid. The principle of SAPF is generating harmonic currents equal in magnitude and opposite in phase to those harmonics. This can keep the grid current in sinusoidal form. Also, connecting the SAPF in shunt with the load enhances the system efficiency and the source power factor (PF) will be much improved.

3 The Control Scheme

The proposed control scheme of the SAPF is shown in Figure 2. The components of this control are explained as follow:

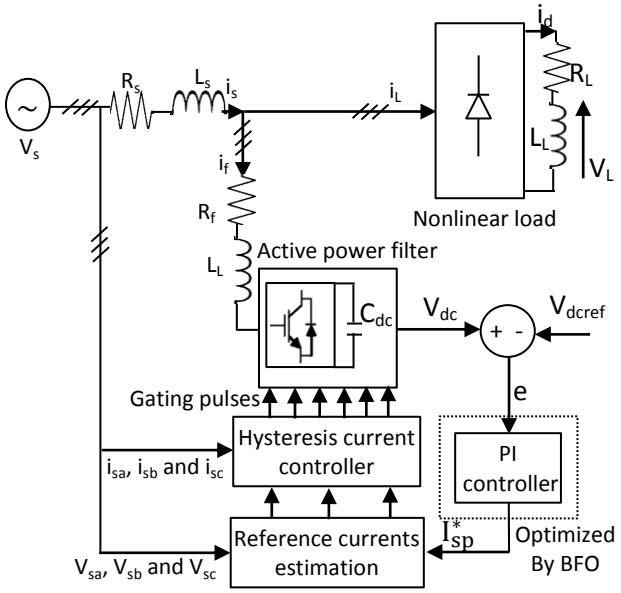

Fig. 2 The system with control scheme of SAPF

3.1 PI Controller

The DC side capacitor voltage is sensed and compared with a reference voltage. This error $e=V_{dcref} - V_{dc}$ is used as an input for PI Controller and the output is the peak value of source current (I^*_{sp}). After I^*_{sp} is obtained, it is multiplied by the unit sine vectors in phase with the respective p.u. source voltages (u_{sa}, u_{sb} and u_{sc}) to obtain the reference source currents (i^*_{sa}, i^*_{sb} and i^*_{sb}). The transfer function of the PI controller is:

$$H(s) = K_p + K_i/S \quad (11)$$

Where, K_p, K_i are the proportional and integral constants respectively. These parameters are traditionally tuned by classical methods such as "Ziegler-Nichols" method which called classical PI controller. This paper presents an artificial intelligent technique for on-line PI controller tuning. This technique is Bacterial Foraging Optimization (BFO).

3.1.1 Bacterial Foraging Optimization

The foraging strategy of *E. coli* bacteria present in our intestines can be explained by four processes, namely Chemotaxis, Swarming, Reproduction, and Elimination and Dispersal [25].

- **Chemotaxis:-** An *E. coli* bacterium can move in two different ways. It can run (swim for a period of time) or tumble and alternates. Swimming and tumbling together are known as chemotaxis.
- **Swarming:-** Swarming of *E. coli* bacterium is to make the bacteria congregate into groups and move as concentric patterns with high bacterial density. This intelligent behavior help the bacteria to reach the richest food location.
- **Reproduction:-** After completion of chemotactic steps, healthier half of the bacteria reproduces to compensate the other half of bacteria which eliminated (poorer foraging abilities). Thus the population of bacteria remains constant in the evolution process.
- **Elimination and Dispersal:-** Unexpected event can occur suddenly during the evolution process. This may eliminate set of the bacteria and disperse them to a new environment.

❖ Bacterial Foraging Algorithm

The steps of the Bacterial Foraging Algorithm (BFA) scheme are given below:

Step1-Initialization

Initialize the parameters p, S, N_s, N_c, N_{re}, N_{ed}, p_{ed}, θ^i,C(i) for (i = *1,2,3, … ,S*) Where,

i. Number of parameters to be optimized (p).
ii. Number of bacteria in the population (S).
iii. Swimming length after the bacteria tumbling in chemotactic loop (N_s).
iv. Number of iteration in the chemotactic loop (N_c), always $N_c > N_s$.
v. Number of reproduction steps (N_{re}).
vi. Number of elimination and dispersal events (N_{ed}).
vii. Probability of the elimination and dispersal bacteria (p_{ed}).
viii. The Location of each bacterium p(i, j, k)= $\theta^i(j, k, l)$ for i = *(1,2,3, … ,S)*.
ix. Step size of the i^{th} bacterium C(i).

Step-2 Iterative Algorithm for Optimization

This Section represents the bacteria population chemotaxis, swarming, reproduction, elimination and dispersal (initially, *j=k=l=0*). For the algorithm updating of (P) lead to updating θ^i automatically.

1) Elimination-dispersal loop: *l=l+1*
2) Reproduction loop :*k=k+1*
3) Chemotaxis loop: *j=j+1*
   a) For *i=1, 2,…, S,* cost function value for each bacterium (*i*) is determined as follows:
      - Calculate cost function value *J(i, j, k, l)* and let
        $J_{sw}(i, j, k, l) = J(i, j, k, l) + J_{cc}(\theta^i(j, k, l), P(j, k, l))$
        Where, ($J_{cc}(\theta)$ is used to model the cell-to-cell attracting for swarming behavior).
      - Let $J_{last} = J_{sw}(i, j, k, l)$ and save this value until finding a better cost through the run.
      - End of For loop.
   b) For *i=1,2,….S,* take the decision of tumbling /swimming.
      i) Tumble: Generate a random vector $\Delta(i) \in \mathcal{R}^p$ with each element $\Delta_m(i)$ *m=1,2,..p.*
      ii) Move: let
      $\theta^i(j+1, k, l) = \theta^i(j, k, l) + C(i)\frac{\Delta(i)}{\sqrt{\Delta^T(i)\Delta(i)}}$
      *iii)*Compute *J(i, j+1, k, l)* and let
      $J_{sw}(i, j+1, k, l) = J(i, j+1, k, l) + J_{cc}(\theta^i(j+1, k, l), P(j+1, k, l))$
      *iv)*Swim:
      Let m=0, (swim length counter).
      - While $m<N_s$
      - Let m=m+1
      - If $J_{sw}(i, j+1, k, l) < J_{last}$, let $J_{last} = J_{sw}(i, j+1, k, l)$ and then $\theta^i(j+2, k, l) = \theta^i(j+1, k, l) + C(i)\frac{\Delta(i)}{\sqrt{\Delta^T(i)\Delta(i)}}$ and use the equation $(\theta^i(j+1, k, l))$ to calculate the new *J(i, j+1, k, l)*
      - Else, let $m=N_s$. (while statement ending).
   c) Go to next bacterium (*i*+1) if *i*≠S (i.e. go to b).
4) If $j<N_c$, go to (3), continue Chemotaxis loop.
5) Reproduction
   a) For k and *l* are given, and for *i=1,2,..S,* let $J^i_{health}=\min\{J_{sw}(i, j, k, l)\}$ be the health of the bacterium *i.* Sort bacteria in order of ascending cost J_{health} (lower health means higher cost).
   b) The $S_r=S/2$ bacteria with highest J_{health} value die and other S_r bacteria with the best value reproduce.
6) If $k < N_{re}$ go to (2), the reproduction steps is not completed, so next generation in the chemotactic loop starts.
7) Elimination-dispersal: To keep the number of bacteria in the population constant, for *i=1,2,..S,* with probability P_{ed}, eliminate and disperse each bacteria to a random location on the optimization domain.

❖ **Flowchart of Bacterial Foraging Optimization**

The flowchart of the Bacterial Foraging Algorithm (BFA) is given in Figure 3.

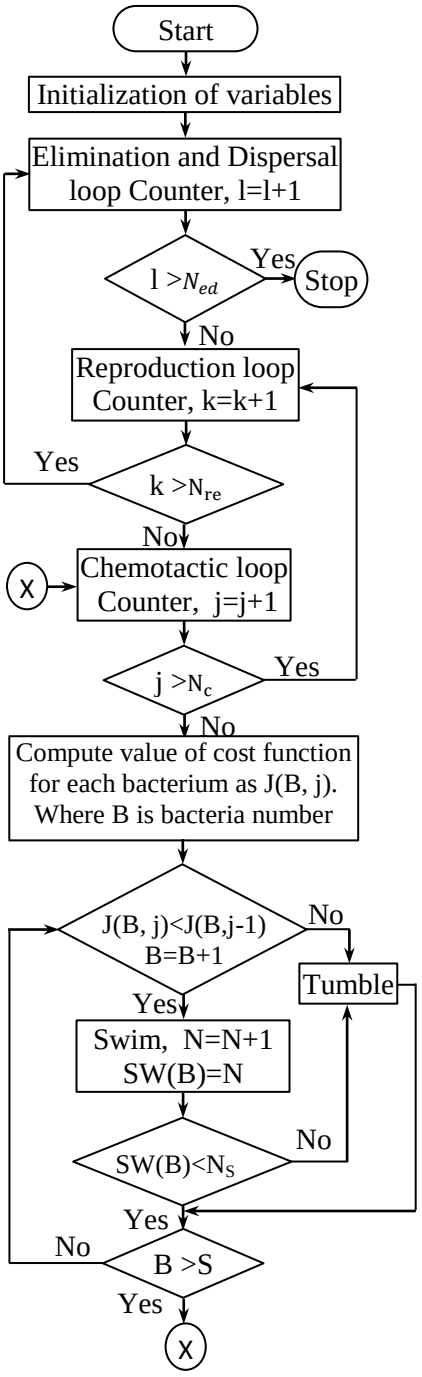

Fig. 3 Flowchart of Bacterial Foraging Optimization

3.2 Reference Source Currents Estimation

The rms source voltage amplitude (V_{sm}) is calculated from the three-phase source voltages (V_{sa}, V_{sb} and V_{sc}) by

$$V_{sm} = \sqrt{\frac{2}{3}(V_{sa}^2 + V_{sb}^2 + V_{sc}^2)} \quad (12)$$

The direct (or in-phase) unit current vectors are given from the three- phase source voltages (V_{sa}, V_{sb} and V_{sc}) and the rms source voltage amplitude (V_{sm}) as expressed in equation 13.

$$\left.\begin{aligned} u_{sa} &= \frac{V_{sa}}{V_{sm}} \\ u_{sb} &= \frac{V_{sb}}{V_{sm}} \\ u_{sc} &= \frac{V_{sc}}{V_{sm}} \end{aligned}\right\} \quad (13)$$

The reference three-phase source currents (i_{sa}^*, i_{sb}^* and i_{sb}^*) are estimated as:

$$\left.\begin{aligned} i_{sa}^* &= I_{sp}^* u_{sa} \\ i_{sb}^* &= I_{sp}^* u_{sb} \\ i_{sc}^* &= I_{sp}^* u_{sc} \end{aligned}\right\} \quad (14)$$

3.3 Hysteresis Non-Linear Current Control

The hysteresis nonlinear current control is the most commonly proposed control method in time domain. This method provides instantaneous current corrective response, good accuracy and unconditioned stability to the system. Also, it aims to keep the controlled current inside a defined rejoin around the desired reference current [9]. In this method, The reference three-phase source currents (i_{sa}^*, i_{sb}^* and i_{sb}^*) are compared with the actual three-phase source currents (i_{sa}, i_{sb} and i_{sc}) to obtain the gating pulses to drive the switching devices of SAPF. The current controller decides the switching pattern of the SAPF devices. The switching logic is determined as follows:

If $i_{sa} < (i_{sa}^* - HB)$ for leg "a" (S_a=1), the upper switch is OFF and the lower switch is ON.

If $i_{sa} > (i_{sa}^* + HB)$ for leg "a" (S_a=0), the upper switch is ON and the lower switch is OFF.
The hysteresis control principle can be shown in figure 4.

The switching functions S_b and S_c that represent pattern of phases "b" and "c" respectively can be determined similarly by the measured currents (i_{sb} and i_{sc}), the corresponding reference currents (i_{sb}^* and i_{sc}^*) and the hysteresis bandwidth (HB).

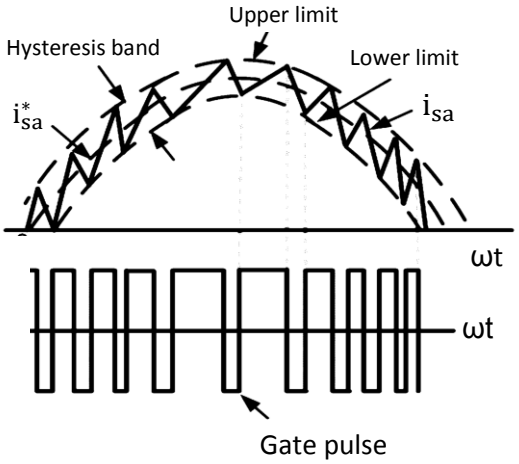

Fig: 4. Hysteresis Control Principle.

4 Objective Function

In this research, the bacterial foraging optimization is used for obtaining the coefficients of PI controller K_P and K_i. The objective in the optimal PI controller design is to mitigate the harmonic currents generated by the nonlinear load in the electric grid. The integral of squared error (ISE) is considered as the cost function to be minimized. The objective function is given by (15).

$$J=\int_0^\infty (e^2)dt \quad (15)$$

Where (J) is the cost function and (e) is the error which evaluated from the following equation.

$$e = V_{dcref} - V_{dc} \quad (16)$$

Therefore, the design problem can be formulated as the following optimization problem.
Minimize J
Subject to

$$Z^{min} \leq Z \leq Z^{max} \quad (17)$$

Where z is a vector, which consists of the parameters of the PI controller. The proposed approach employs BFO to search for the optimal set of PI controller coefficients which leads to minimizing the total harmonic distortion.

5 Simulation Results and Discussions

The proposed system parameters are obtained in Appendix. There are some assumptions and suggestions must be cleared. The switching device of the inverter is IGBT-transistor. The actual model of IGBT -as a switch- is included and the setting parameters of the switch are also tabulated in appendix. Also, the effect of the heat on the overall system parameters is neglected. In addition, the same algorithm is used in simulation for both PI-classical and PI-BFO controllers without any extra cost.

5.1 The System Results Without SAPF

Figure 5 represents the sinusoidal three-phase source voltages. Figure 6 shows the source phase current without using SAPF and in the same time it represents the load phase current without using SAPF.

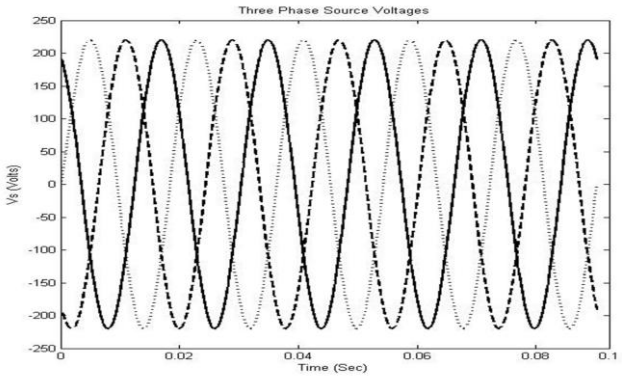

Fig. 5 Three-phase source voltages

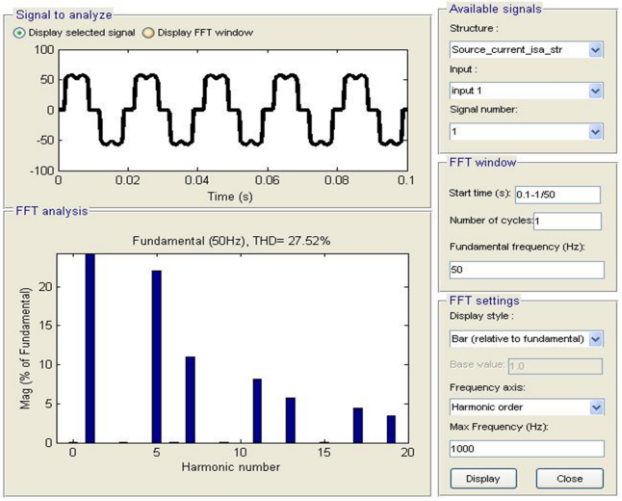

Fig. 6 The phase source current (i_{sa})

However, due to the non-linear, the source current is distorted and the overall total harmonic distortion (THD) is equal to (THD =27.52%). These results obtained in figures 6 are calculated by using Fast Fourier Transform (FFT).

$$\text{THD}=\sqrt{\sum_{n=2}^{\infty} i_n^2}\Big/ i_1 \qquad (18)$$

Where, i_n, i_1 are the RMS value of nth order harmonic and fundamental frequency of currents respectively.

5.2 The SAPF Results With Classical PI Controller

Then, the system is controlled by classical PI controller where the parameters of the "Ziegler-Nichols" formula are (K_P = 0.1 and K_i = 0.4). The results show that the waveform of the phase source current is improved and dependently THD is reduced to 7.37%.

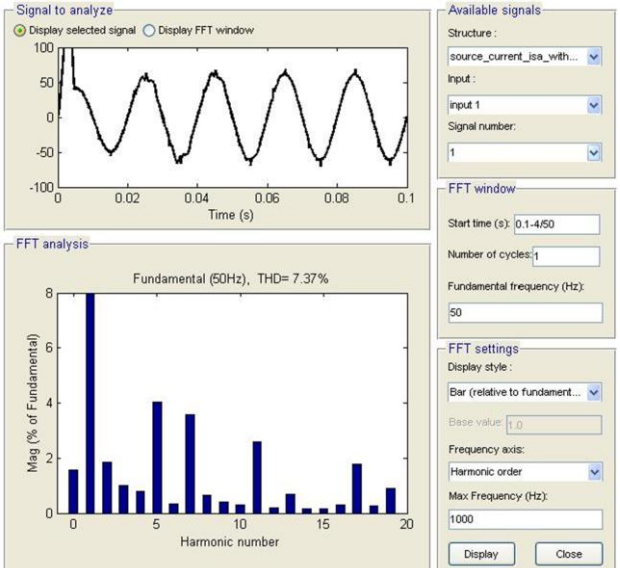

Fig. 7 The phase source current (i_{sa})

5.3 The Results of PI-BFO Controlled SAPF

Most researches have suggested off-line tuning for the PI controller parameters. But this proposed research uses tow S-functions in matlab/Simulink software package for on-line self-tuning self-adaptive algorithms. The process of on-line tuning for the parameters of PI controller can be observed through figures 8 and 9.

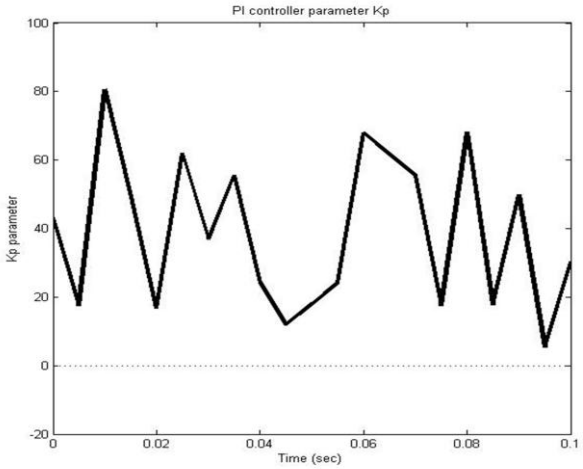

Fig. 8 On-line tuning of controller gain (K_p)

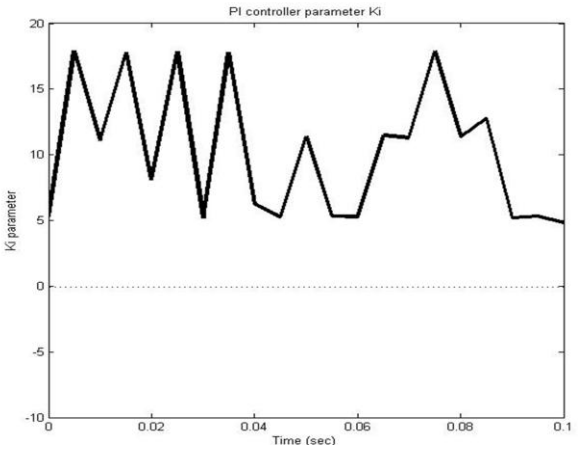

Fig. 9 On-line tuning of controller gain (K_i)

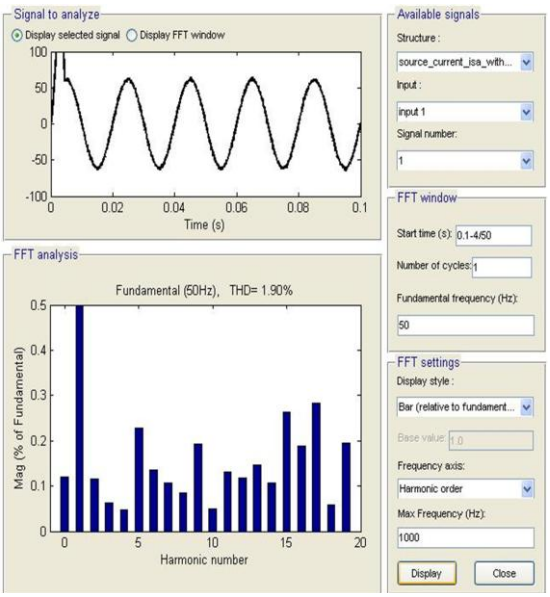

Fig. 10 The source phase current (i_{sa}) BFO-SAPF

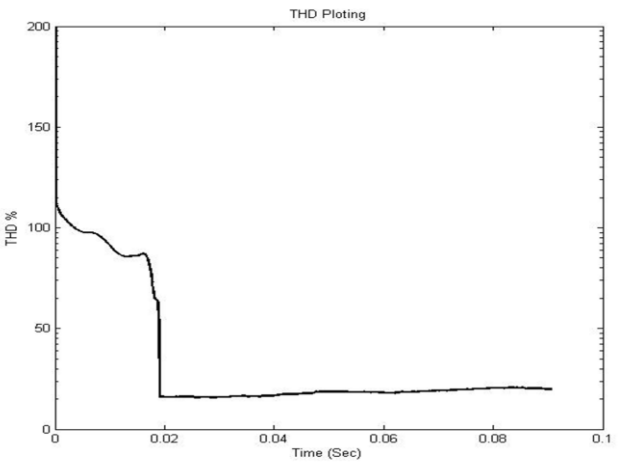

Fig. 11 THD for on-line BFO tuning

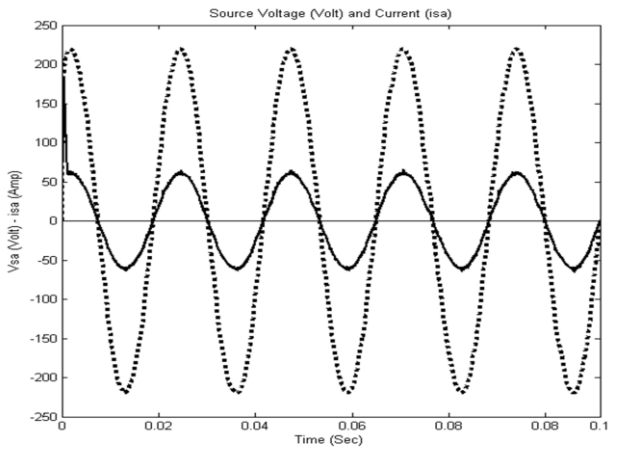

Fig. 12 The source voltage (V_{sa}) and current (i_{sa}) with APF Based PI-BFO

The results-from figures 10 and 11- show that there are marked improvement in the system behavior when using SAPF that controlled by on-line BFO tuning. THD was reduced to 1.90 % and the power factor was approximately reached unity as shown in figure 12. In this figure both voltage and current waveforms are approximately in phase, and there is no phase shift between them. However, the SAPF based on-line BFO has strong effectiveness for harmonics mitigation and improvement the power system quality instead of classical PI controller.

6 Conclusions

In this paper, the proposed SAPF uses an intelligent control algorithm that depends on the BFO. This

proposed controller is known as PI-BFO. The system that includes non-linear distorted load is simulated without SAPF and then simulated PI-SAPF classical controller. The results demonstrate that the THD of the supply phase current is 27. 52% without SAPF. Also, the THD is reduced to 7.37% when using classical PI controller. But, on the opposite side, the performance of the system with the proposed SAPF controlled by on-line tuning PI-BFO controller is improved and the harmonic due the non-linear load is eliminated. In addition, THD is minimized to 1.9% and the supply power factor is approximately unity.

Finally, the proposed SAPF with PI-BFO controller is robust, reliable and contributes to wards harmonic mitigation, PF correction and power quality enhancement of electric grid.

***References*:**

[1] B. Singh, K. Al-Haddad and A. Chandra, "A new control approach to three-phase active filter for harmonics and reactive power compensation", *IEEE Transactions on Power Systems*, Vol. 13, No. 1, pp. 133-138, February 1998.

[2] Z. Chen, Y. Luo and M. Chen, "Control and performance of a cascaded shunt active power filter for aircraft electric power system", *IEEE Transactions on Industrial Electronics*, Vol. 59, No. 9, pp. 3614-3623, September 2012.

[3] Q. Trinh and H. Lee, "An advanced current control strategy for three phase shunt active power filters", *IEEE Transactions on Industrial Electronics*, Vol. 60, No. 12, pp. 5400-5410, December 2013.

[4] A. F. Zobaa, "Optimal multi-objective design of hybrid active power filters considering a distorted environment", *IEEE Transactions on Industrial Electronics*, Vol. 61, No. 1, pp. 107-114, 2014.

[5] P. Acuna, L. Moran, M. Rivera, J. Dixon and J. Rodriguez, "Improved active power filter performance for renewable power generation systems", *IEEE Transactions on Power Electronics*, Vol. 29, No. 2, pp. 687-694, February 2014.

[6] H. Akagi, "New trends in active filters for improving power quality", *IEEE-PEDES Conference Record*, pp. 417-425, January 1996.

[7] H. Akagi, Y. Kanazwa and A. Nabae, "Instantaneous reactive power compensators comprising switching devices without energy storage components", *IEEE Transactions on Industry Applications*, Vol. IA-20, No. 3, pp. 625-630, May/July 1984.

[8] S. Bhattacharya, A. Veltman, D. M. Divan and R. D. Lorenz, "Flux based active filter controller", *IEEE-IAS Annual Meeting*, pp. 2483-2491, 1995.

[9] M. Rastogi, N. Mohan and A. A. Edris, "Hybrid active filtering of harmonic currents in power systems", *IEEE Transactions on Power Delivery*, Vol. 10, No. 4, pp. 1994-2000, October, 1995.

[10] K. M. Passino, "Biomimicry of bacterial foraging for distributed optimization and control", *IEEE Control Systems Magazine*, Vol. 22, No. 3, pp. 52–67, June 2002.

[11] S. Dasgupta, S. Das, A. Abraham and A. Biswas, "Adaptive computational chemotaxis in bacterial foraging optimization: an analysis", *IEEE Trans. on Evol. Comp.*, Vol. 13, Issue: 4, pp. 919-941, 2009.

[12] S. Mishra, C. N. Bhende, L. L. Lai, "Optimization of a distribution static compensator by bacterial foraging technique", *IEEE Conf. on Machine Learning and Cybernetics, Dalian, China*, pp. 4075-4082, 13-16 August 2006.

[13] S. Mishra, "A Hybrid least square-fuzzy bacterial foraging strategy for harmonic estimation", *IEEE Transactions on Evolutionary Computation*, Vol. 9, No. 1, pp. 61-73, February 2005.

[14] S. Mishra, C. N. Bhende, "Bacterial foraging technique-based optimized active power filter for load compensation", IEEE Transactions on Power Delivery, Vol. 22, No. 1, 2007, pp. 457-465.

[15] M. Tripathy, S. Mishra, G. K. Venayagamoorthy, "Bacterial foraging: a new tool for simultaneous robust design of UPFC controllers", *IEEE Conf. on Neural Networks, Vancouver, BC, Canada*, pp. 2274-2280, 16-21 July 2006.

[16] M., Tripahty, S. Mishra, "Optimizing voltage stability limit and real power loss in a large power system using bacterial foraging", *IEEE Conf. on Power Eectronics and Energy Systems, New Delhi*, pp.1-6, 12-15 December 2006.

[17] S. Mishra, M. Tripahty, J. Nanda, "Multi-machine power system stabilizer design by rule based bacterial foraging", *Electric Power Systems Research*, Vol.77, pp.1595-1607, 2006.

[18] M. Tripahty, S. Mishra, "Bacterial foraging-based solution to optimize both real power loss and voltage stability limit", *IEEE Transactions on Power Systems*, Vol. 22, No. 1, pp. 240-248, February 2007.

[19] B. Sumanbabu, S. Mishra, B. K. Panigrahi, G. K. Venayagamoorthy, "Robust tuning of modern power system stabilizers using bacterial foraging algorithm", *IEEE Conf. on Evol. Comp.*, pp. 2317-2324, 25-28 2007.

[20] M. A. Munoz, S. K. Halgamige, W. Alfonso, E. F. Caicedo, "Simplifying the bacterial foraging optimization algorithm", *IEEE Conf. on Evolutionary Computation, Barcelona*, pp. 1-7, 18-23 July 2010.

[21] E. Daryabeigi, M. Moazzami, A. Khodabakhshian, M. H. Mazidi, "A New power system stabilizer design by using smart bacterial foraging algorithm", *IEEE Candian Conf. on Elect. Comp. Engineering, Niagara Falls*, pp. 713-716, 8-11 2011.

[22] H. E. E. Bayoumi, "Minimal overshoot direct torque control for permanent magnet synchronous motors using hybrid bacterial foraging-particle swarm optimization", *IEEE Conf. on Comp. Intelligence in Cont. and Autom., Singapore*, pp. 112-119, 2013.

[23] S. Mishra, "A Hybrid least square-fuzzy bacterial foraging strategy for harmonic estemation", *IEEE Transactions on Evolutionary Computation*, Vol. 9, No. 1, pp. 61-73, February 2005.

[24] S. Mishra, C. N. Bhende, "Bacterial foraging technique-based optimized active power filter for load compensation", *IEEE Transactions on Power Delivery*, Vol. 22, No. 1, pp. 457-465, January 2007.

[25] H. I. Abdul-Ghaffar, E. A. Ebrahim, M. Azzam, "Design of PID controller for power system stabilization using particle swarm-bacterial foraging optimization", *WSEAS Transactions on Power Systems*, Vol. 8, Issue 1, pp. 12-23, January 2013.

Appendix

- The IGBT parameters:

	Parameter	Value
1	Internal Resistance, R_{on}	1e-3 Ω
2	Snubber Resistance, R_s	1e5 Ω
3	Snubber Capacitance, C_s	Inf

- The system parameters:

	Nonlinear system parameters	Value
1	Three phase source voltage, V_s	220 V
2	Frequency, f	50 Hz
3	Source resistance, R_s	0.1Ω
4	Source inductance, L_s	0.15mH
5	Load resistance, R_l	6.7Ω
6	Load inductance, L_l	2mH
7	Filter resistance, R_f	0.1Ω
8	Filter inductance, L_f	0.335mH
9	DC Capacitance, C_{dc}	2200 µF
10	DC Reference Voltage, V_{dc}	850 V

- The Bacterial Foraging Optimization parameters:

1	Dimension of the search space (p)	2
2	No. of bacteria in the population (S)	6
3	Swimming length (N_s)	4
4	No. of chemotactic steps (N_c)	4
5	No. of reproduction steps (N_{re})	100
6	No. of elimination events (N_{ed})	2
7	Probability of eliminated bacteria (P_{ed})	0.25
8	No. of bacteria of best cost function (S_r)	S/2